AIAC-2013-056

MODELING AND SIMULATION OF COAXIAL-ROTOR HELICOPTER AERODYNAMICS IN HOVER AND FORWARD FLIGHT

Murat Gecgel[1]
Turkish General Staff
Ankara, Turkey

Oktay Baysal[2]
Old Dominion University
Norfolk, VA, USA

ABSTRACT

The present investigation aims to develop a framework for the computational analyses of a coaxial helicopter rotor flow field in hover and in forward flight. The methodology is based on the unsteady solutions of the three-dimensional, compressible Navier-Stokes equations recast in a rotating frame of reference. The simulations are carried out by solving the developed mathematical model on hybrid meshes that aim to optimally exploit the benefits of both the structured and the unstructured grids around complex configurations. The computer code is prepared for parallel processing with distributed memory utilization in order to significantly reduce the computational time and the memory requirements. The developed model and the simulation methodology are validated for single rotor flowfields by comparing the present results with the published experimental data for hovering. The predictive merit of different turbulence models for complex helicopter aerodynamics has been tested extensively. It was deemed best to use the one-equation Spalart-Allmaras turbulence model for the subsequent rotor flowfield computations. Firstly, the flowfield around a single rotor in forward flight is simulated. These time–accurate computations help to analyze an adverse effect of increasing the forward flight speed. A dissymmetry of the lift on the advancing and the retreating blades has been observed for different advance ratios. Since the coaxial rotor is proposed to mitigate the dissymmetry, it is selected as the next logical step of the present investigation. The time–accurate simulations are successfully obtained for the flowfields generated by first a hovering then a forward-flying coaxial rotor. The results for the coaxial rotor in forward flight verify the aerodynamic balance proposed by the previously published advancing blade concept. The final set of analyses aims to investigate if the gap between the two rotors of the coaxial configuration has any significant effect on the generated forces. The present results indicate either little or no such effect on the lift.

INTRODUCTION

A helicopter is a complex air vehicle that has rotating surfaces to provide lift, propulsion, and control forces. These forces are created on the spinning blades and they enable a helicopter to have a unique manoeuvring capability. The power from an engine is transmitted to the rotor shaft to turn the rotor. Basically, there are four flight regimes in which a helicopter operates. The first is hover, where the thrust produced by the spinning blades exactly offsets the weight of the helicopter. The helicopter remains stationary at some height over the ground. The second one is vertical climb where additional thrust is needed to move the helicopter upward. Vertical descent, the third is quite complicated due to the effects of both upward and downward flows through the rotor disk, which may cause blade vibration. In forward flight, the last one, rotor disk tilts forward in the direction of the flight to create the thrust to overcome the drag. This flight capabilities have a high price like mechanical and aerodynamic complexity and high power requirements [Leishman, 2006].

The accurate prediction of the flows around hovering and forward flying helicopter rotors is a challenging problem due to the difficulties like blade-vortex interaction (BVI), vibration, interaction with the tail rotor, effects of the helicopter body, ground effect and the flow induced by the rotor alone [Sheffer et al., 1997]. Many authors have undertaken the numerical simulation of flows around hovering helicopter rotors [Pomin and Wagner, 2001; Srinivasan et al., 1991; Rouzaud et al., 1997; Caradonna and Tung, 1981; Le Pape and Beaumier, 2005]. Successful results have been reported for

[1] Dr.Lt.Col. in Turkish General Staff, Email: mgecgel@ae.metu.edu.tr
[2] Prof. in Department of Mechanical and Aerospace Engineering, Email: obaysal@odu.edu

the prediction of the flow fields around forward flying single rotors [Allen, 2007; Stejil et al., 2006; Strawn and Biswas, 1994; Xu et al., 2005; Yang et al., 2000]. Furthermore, forward flight simulations including the periodic motion of the blades have been undertaken by few researchers [Altmikus et al., 2002; Servera et al., 2001; Park and Kwon, 2004; Boelens et al., 2002; Van der Ven and Boelens, 2004]. A detailed account of all aerodynamic challenges related to the analysis of helicopter rotors is described in the review paper of Conlisk (2001).

However, the effect of dynamic stall on a retreating blade is still a challenging problem for high forward flight speeds. Once a conventional helicopter is in forward flight, dissymmetry of lift imposes a upper speed limit. While the advancing blade(s) travels at transonic or even supersonic speeds, the retreating blade(s) moves much slower to enter the stall condition and to fail to produce lift. Coaxial rotors may solve the problem of dissymmetry of lift because one set of rotors is cancelled by the corresponding increased lift on the same side of the other set of rotors, and vice versa. Eventually, a coaxial design can fly (theoretically) faster than a conventional one. Furthermore, it will be more stable in the extreme parts of the flight envelope. Although there are a few helicopters in service with coaxial rotors, a computational model to analyze the interaction of the flows generated by the two rotors has not been yet reported. Moreover, a parametric study to achieve better coaxial rotor designs cannot be found at least in the open literature.

The objectives of this investigation can be listed as;

- Validate of the presently constructed mathematical and computational methodologies for rotorcraft aerodynamics within the limitations of the data available
- Evaluate computational simulation of the flowfield around a single-rotor in hover then in forward flight
- Extend the computational model to coaxial rotorcraft in hover then in forward flight
- Study the effects of rotor seperation distance on the produced lift
- Verify “the aerodynamic symmetry in forward flight” proposed by the “Advancing Blade Concept” [Cheney, 1969; Coleman, 1997]

METHODOLOGY

The Navier–Stokes Equations are the most general description of the fluid flow in thermodynamic equilibrium. It is basically the collection of the conservation of mass, the conservation of momentum and the conservation of energy equations written for a Newtonian fluid. The integral form, which is also the basis of all finite volume algorithms, can be written as,

$$\frac{\partial}{\partial t}\int_{\Omega}\vec{q}\,d\Omega + \oint_{S}\vec{F}\cdot d\vec{S} = 0$$

The differential form can be written as,

$$\frac{\partial \vec{Q}}{\partial t} + \frac{\partial\left(\vec{E}-\vec{E}_v\right)}{\partial x} + \frac{\partial\left(\vec{F}-\vec{F}_v\right)}{\partial y} + \frac{\partial\left(\vec{G}-\vec{G}_v\right)}{\partial z} = 0$$

Numerical Method of Solution

The present investigation incorporated in its toolkit is a commercially available solver, FLUENT. This code solves numerically the compressible, mass-weighted, Reynolds-averaged Navier-Stokes (RANS) equations with several turbulence models. The results have been obtained by running the code on the UNIX clusters (Wilbur & Zorka) located at Old Dominion University. In order to reduce the computational efforts, parallel processing has been utilized, where the data communication has been achieved via MPI (Message Passage Interface) libraries. The simulations have been performed by employing unsteady, density-based solver with implicit dual-time-stepping scheme (2^{nd} order of accuracy). The third order MUSCL **(**Monotone Upstream-Centered Schemes for Conservation Laws**)** scheme has been applied for spatial discretization**.** This third-order convection scheme was conceived from the original by blending a central differencing scheme and second-order upwind scheme. Compared to the second-order upwind scheme, the third-order MUSCL has a potential to improve spatial accuracy for all types of meshes by reducing numerical diffusion, most significantly for complex three-dimensional flows, and it is available for all transport equations [Fluent 6.3 User’s Guide, 2006]. Courant number has been ramped up to five. The solver provides an efficient Moving Mesh technique. The mesh has been rotated with an angular velocity which corresponds to the tip Mach number, M_{tip}, encountered for a given case. A uniform computational time step of $\delta t=1x10^{-5}$ (e.g., 473 steps for 1 revolution, Ω=132.9 rad/s) has been used for the simulations.

Validation of the Methodology

The validation methodology has been performed using the experimental data obtained by Caradonna and Tung in 1981. This test case is extensively used by the helicopter community for the validation of CFD codes applied to rotorcraft problems. The test cases range from simple, two-bladed, non-lifting rotors of simple plan-form, to lifting cases with high tip Mach numbers. Caradonna and Tung [1] carried out an experimental and analytical study of a model helicopter rotor in hover. The experimental study involved simultaneous blade pressure measurements and tip vortex surveys. The model rotor consists of two rectangular, untwisted and untapered NACA-0012 rigid blades mounted on a tall column containing a drive shaft located in a large chamber with special ducting designed to eliminate room recirculation. The rotor aspect ratio, defined as the ratio of rotor radius and blade chord was six. The model rotor for CFD simulations had a diameter of 2.286 m, and a chord length of 0.191 m. The computational model utilizes flat tip surfaces and sharp trailing edges for all blades. A large set of test conditions has been applied with the tip Mach number ranging from M_{tip}=0.226 to M_{tip}=0.890 and the collective pitch setting of $\theta=0^o$ to 12^o at ambient conditions. Pressure distributions have been measured at five span wise cross-sections (r/R=0:50, 0.68, 0.80, 0.89 and 0.96) of the blade and tip vortex trajectory has been extracted using a hotwire technique. The modeled geometry of the Caradonna-Tung rotor is shown in (Figure 1).

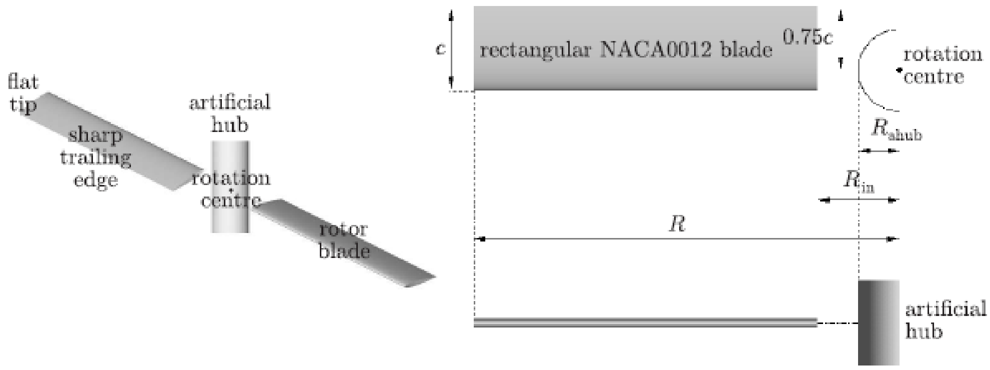

Figure 1: *Caradonna - Tung rotor blade ($\alpha=0^o$, AR=6, R_{ahub}=0.5c, R_{in}=c, R=6c)*

<u>Grid Generation for Validation Cases:</u>

After having unsatisfactory results by employing unstructured grids, hybrid grid technique has been utilized for generation of computational mesh. Firstly, a structured mesh block consists of hexahedral cells around the rotor has been created. The structured block is H-type in stream wise and span wise directions while it is O-type in normal direction. There are 41x41x41 grid points in stream wise, span wise and normal directions, respectively. Then, the rest of the domain has been filled with tetrahedral, prismatic, and pyramid elements. The hybrid mesh consists of 288,000 hexahedral and 990,704 mixed cells. Details of computational mesh are displayed in (Figures 2 and 3).

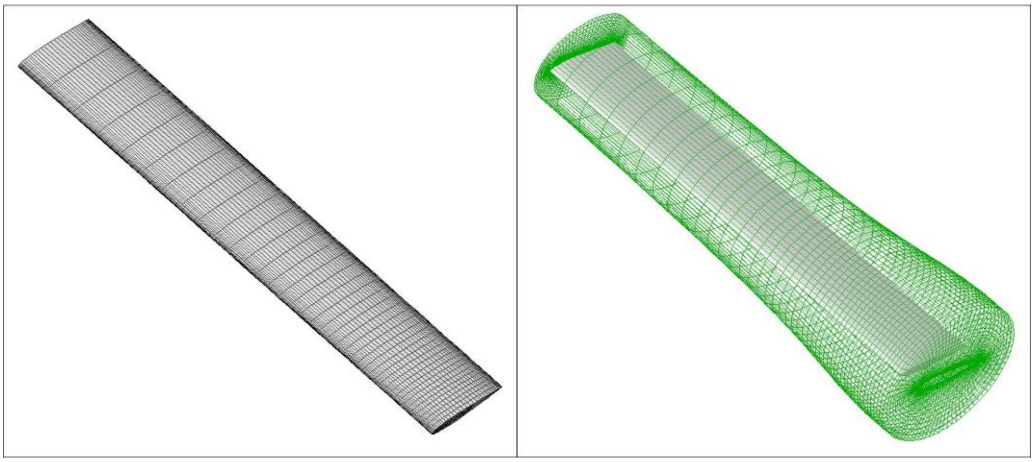

Figure 2: *Grid points on the modeled blade surface (left) and structured block around Caradonna - Tung rotor blade (right)*

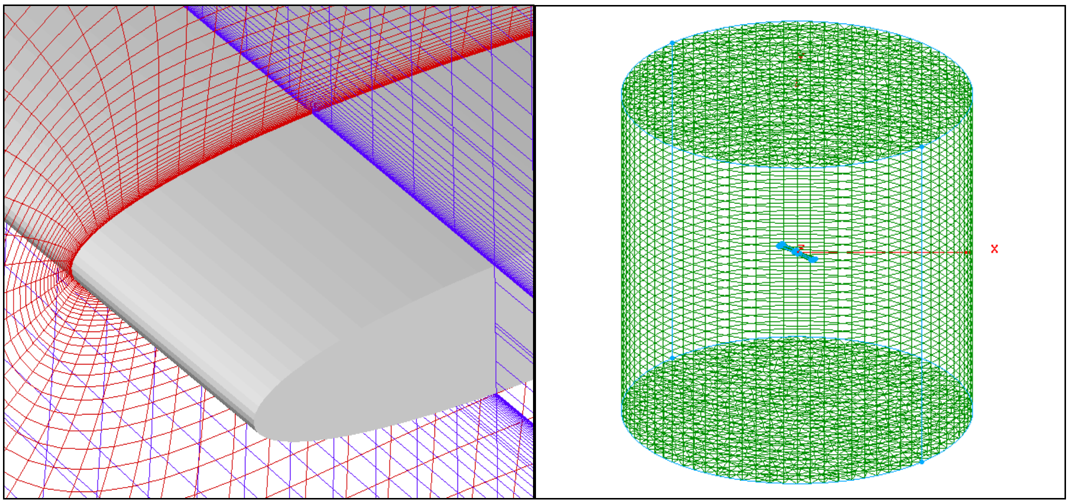

Figure 3: *Mesh topology near tip region (left) and hybrid block around the rotor (right)*

<u>Results of Validation Cases:</u>

A detailed insight into the flow behavior may be obtained by comparing the pressure coefficient, C_p distribution with the experimental data at three cross-sections along the span of the blade (r/R=0.5, 0.80 and 0.96). For this purpose, laminar and inviscid simulations have been carried out for non-lifting and lifting rotor configurations. For the non–lifting cases, computations have been performed by setting the angular velocity to 132.9 rad/s, which corresponds to a tip Mach number, M_{tip}=0.52 and a rotor tip velocity, U_{tip} =176.8 m/s. For the lifting cases, collective pitch angle has been set to 8^o. The simulations have been performed for a subsonic tip Mach number, M_{tip}=0.439 (Ω=112.2 rad/s, U_{tip}=149.26 m/s) and a transonic tip Mach number, M_{tip}=0.877 (Ω=224.2 rad/s, U_{tip}=298.2 m/s).

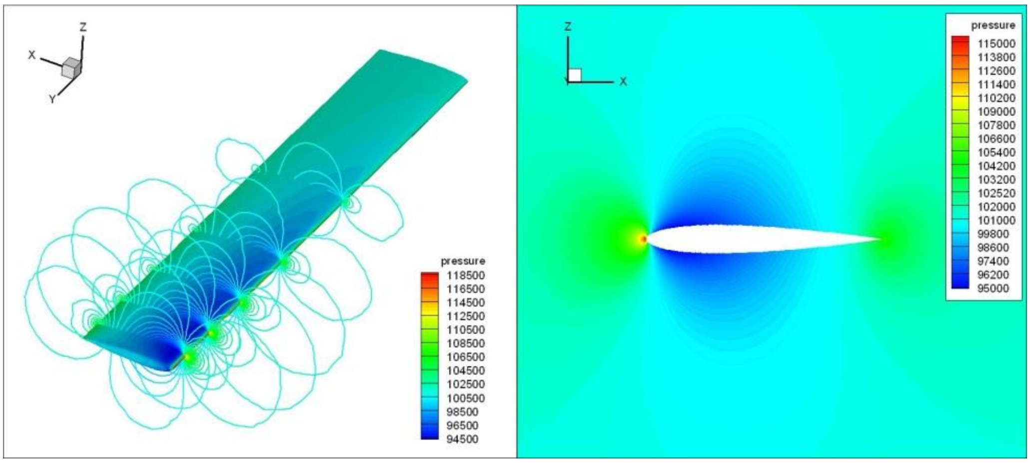

Figure 4: *Pressure contours at 5 (r/R=0.5, 0.68, 0.80, 0.89 and 0.96) span wise stations (left) and pressure contours at r/R=0.89, inviscid, hover, Ω=132.9 rad/s, M_{tip}=0.52, α=0°, Re=2.47x10^6 (right)*

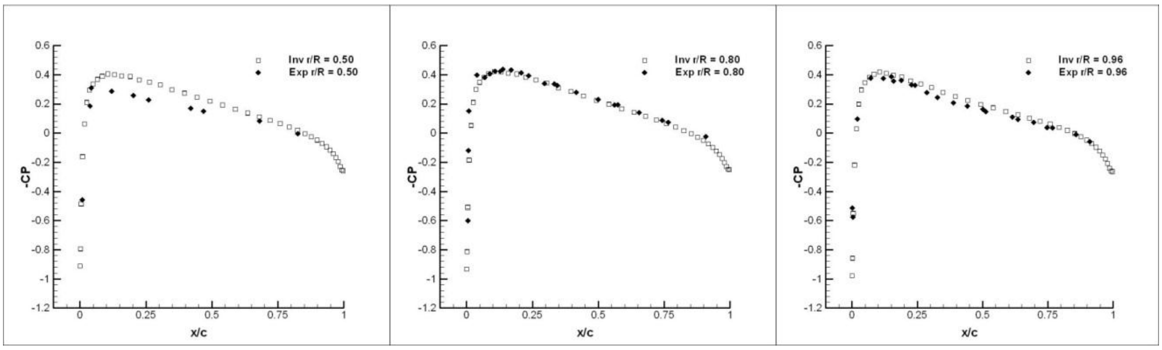

Figure 5: *Comparison of C_p distributions at 3 span wise stations (r/R=0.5, 0.80 and 0.96), inviscid, hover, α=0°, M_{tip}=0.52*

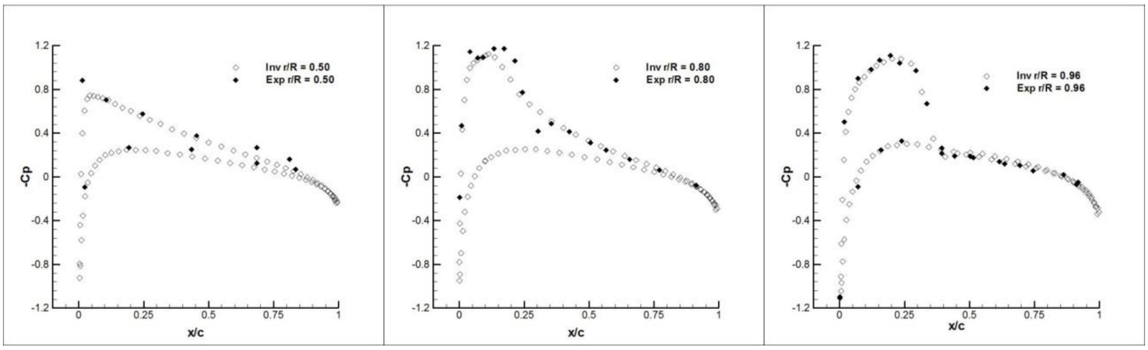

Figure 6: *Comparison of C_p distributions at 3 span wise stations (r/R=0.5, 0.80 and 0.96), inviscid, hover, α=8°, M_{tip}=0.877*

The figures demonstrate the good agreement obtained between the computed and measured surface pressure distributions. It is noteworthy that the shock location is predicted correctly in accordance with the measurements for all transonic cases. The overall agreement with the experimental data is satisfactory. Therefore, the methodology has been deemed as validated successfully and can be used for more complex computations.

Determination of Turbulance Model

It is an unfortunate fact that no single turbulence model is universally accepted as being superior for all classes of problems. The choice of turbulence model will depend on considerations such as the physics encompassed in the flow, the established practice for a specific class of problem, the level of accuracy required, the available computational resources, and the amount of time available for the simulation. To make the most appropriate choice of model for a given application, one needs to understand the capabilities and limitations of the various options. Therefore, several turbulence models have been utilized and tested for the simulation of a case where α=8^o, M_{tip}=0.877. Results have been compared with experimental data. The aim is to investigate which turbulence model works best for the present helicopter simulations.

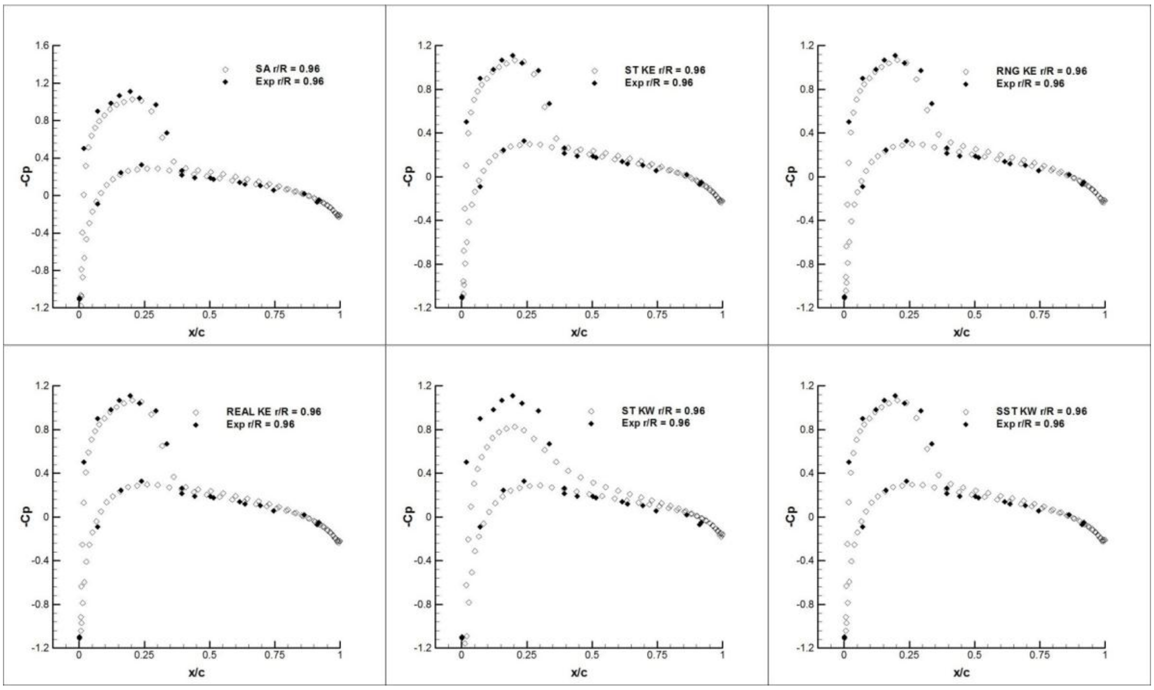

Figure 7: *C_p predictions of several turbulence models at 3 span wise stations (r/R=0.5, 0.80 and 0.96), hover, α=8^o, M_{tip}=0.877*

It has been observed that the overall CFD results show good agreement with experimental data. However, while the pressure values computed by employing Spalart–Allmaras, The Standart *k–ε,* RNG *k–ε, Realizable k–ε* and SST *k–ω* turbulence models seem to be identical to the experimental data, the predictions of The Standart *k–ω* and LES models are not as accurate as the other models. In CFD computations, the level of accuracy required and the available computational resources are quite important and have to be considered carefully. As the number of equations to be solved increases, the computational cost will also increase too. Among the models tested, Spalart-Allmaras is the only one-equation model. Therefore, it is the cheapest model by means of computational cost. Hence, Spalart-Allmaras turbulence model has been chosen and employed in the entire simulations.

Computational Domain and Grid Topology for Coaxial Rotor Configuration

The structured blocks consist of hexahedral cells around the rotors. The structured blocks are H-type in stream wise and span wise directions while it is O-type in normal direction. There are 41x41x41 grid points in stream wise, span wise and normal directions, respectively. For coaxial rotor simulations, 3 structured blocks have been generated for each rotor.

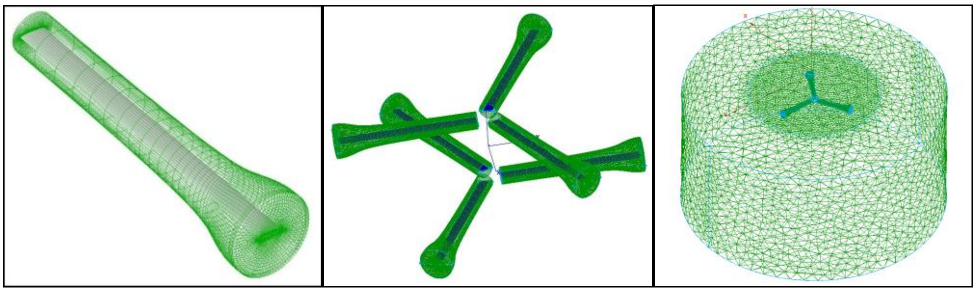

Figure 8: *Computational Mesh Used in Coaxial Rotor Simulations*

In the next step, the rotors have been placed in the lower and upper blocks. The rest of the block domain has been filled with tetrahedral, prismatic, and pyramid elements. Each hybrid block consists of 432,000 hexahedral and 864,000 mixed cells (total 1,045,109 cells).The upper and lower rotors have been rotated in opposite directions. While the lower rotor (and its block) has been rotated in the counter clockwise direction with an angular velocity of Ω=60 rad/s, the angular velocity of upper rotor (block) has been set to -60 rad/s. This rotation has been achieved via moving and sliding mesh techniques. In the sliding mesh technique two or more cell zones are used. (If one generates the mesh in each zone independently, one would need to merge the mesh files prior to starting the calculations). Each cell zone is bounded by at least one "interface zone" where it meets the opposing cell zone. The interface zones of adjacent cell zones are associated with one another to form a "grid interface." The two cell zones move relative to each other along the grid interface. During the calculations, the cell zones slide (i.e., rotate or translate) relative to one another along the grid interface in discrete steps. As the rotation or translation takes place, node alignment along the grid interface is not required. Since the flow is inherently unsteady, a time-dependent solution procedure is required. To compute the interface flux, the intersection between the interface zones is determined at each time step. The resulting intersection produces one interior zone (a zone with fluid cells on both sides) and one or more periodic zones. If the problem is not periodic, the intersection produces one interior zone and a pair of wall zones, which is empty if the two interface zones intersect entirely. Therefore, these wall zones are changed to another appropriate boundary type. The resultant interior zone corresponds to where the two interface zones overlap and the resultant periodic zone corresponds to where they do not. The number of faces in these intersection zones varies as the interface zones move relative to one another. The fluxes across the grid interface are computed using the faces resulting from the intersection of the two interface zones, rather than from the interface zone faces themselves [Fluent 6.3 User's Guide, 2006]. The surface between lower and upper blocks has been defined as "interface" and divided into two parts. The inner part has a higher resolution since the crucial part of data communication occurs on this surface.

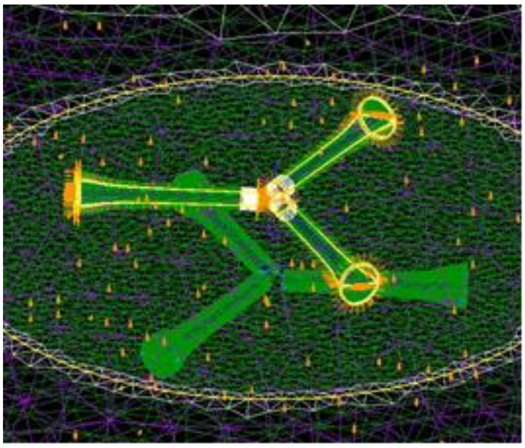

Figure 9: *Lower and upper rotors and inner interface surface between rotor blocks*

RESULTS

While a conventional (a single-rotor) helicopter is in forward flight, an aerodynamic dissymmetry develops on the rotor blades. It imposes an upper speed limit upon single-rotor helicopters. On the advancing side of the rotor disc, rotor blades travel through the air sufficiently quickly for the airflow over them to become transonic or even supersonic, while on the retreating side of the rotor disc, the rotors travel through the air much more slowly, possibly slowly enough to enter the stall condition. As a result, these aerodynamic conditions result in flight instability. Before going through the coaxial rotor forward flight analysis, observing and analyzing the development of aerodynamic dissymmetry on the forward flying single rotors will prove to be a useful preparation. The forward flight cases are the simulations of the flows around isolated model helicopter rotors in forward flight without a pitching or flapping motion. The blades are considered to have NACA 0012 sections with an angle of attack, $\alpha=8^0$. Spalart–Allmaras turbulence model has been utilized for all forward flight cases.

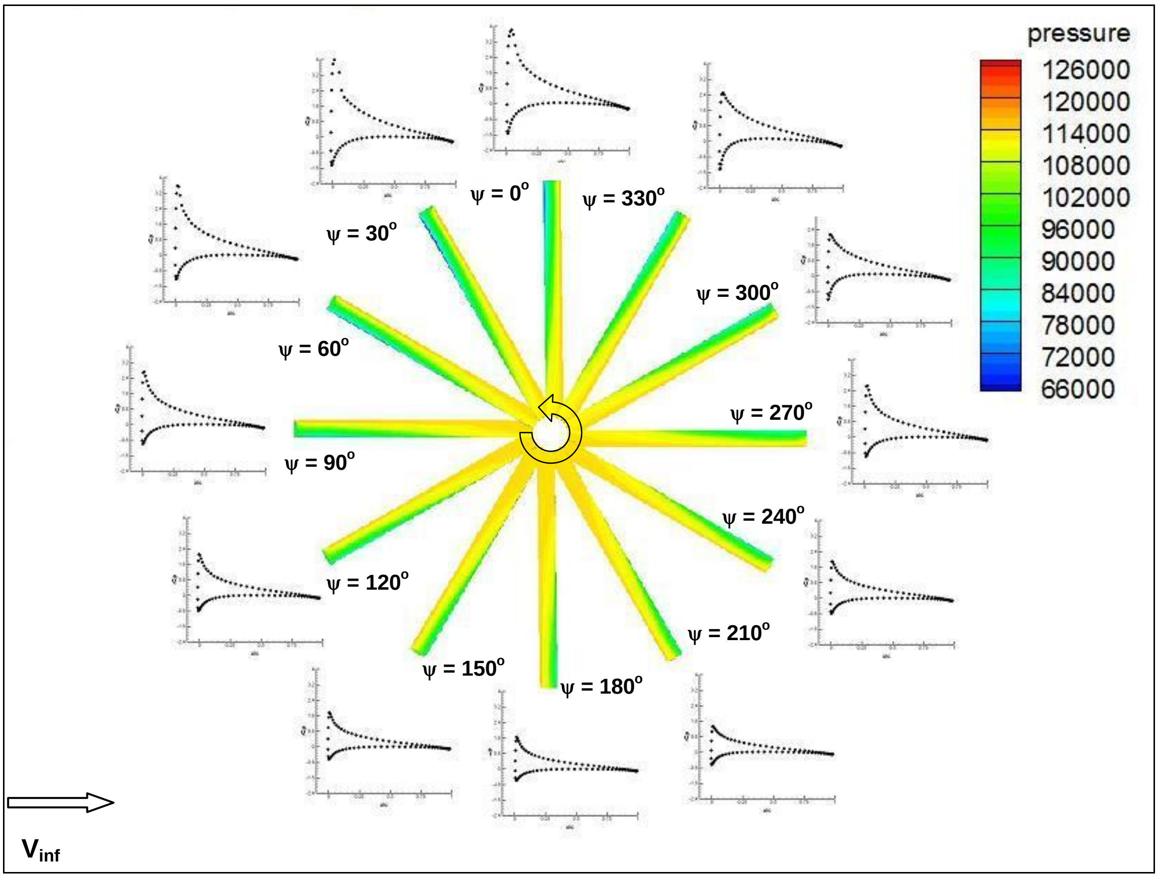

Figure 10: *Surface pressure contours and C_p distributions (r/R=0.89) at different azimuth angles, Spalart–Allmaras, forward flight, η=0.2, M_{tip}=0.52, $\alpha=8^o$*

As mentioned above, the most important superiority of coaxial rotor configuration against conventional (single rotor) rotor configuration is the high forward speed achieved via balanced lift by counter rotating lower and upper rotors. In this study, verification of aerodynamic symmetry proposed by coaxial rotor design has been intended. For this purpose, the hybrid grid generated for L3 (H/D=0.2) case has been utilized. The angular velocity of lower and upper rotors have been set to Ω_{low}=60 rad/s and Ω_{upp}=-60 rad/s, respectively. 7 forward flight cases have been performed by setting the advance ratio (η) to 0.1, 0.2, 0.3, 0.4, 0.5, 0.6 and 0.7. Figures 11-17 display the pressure contours at different time steps for 7 different advance ratios.

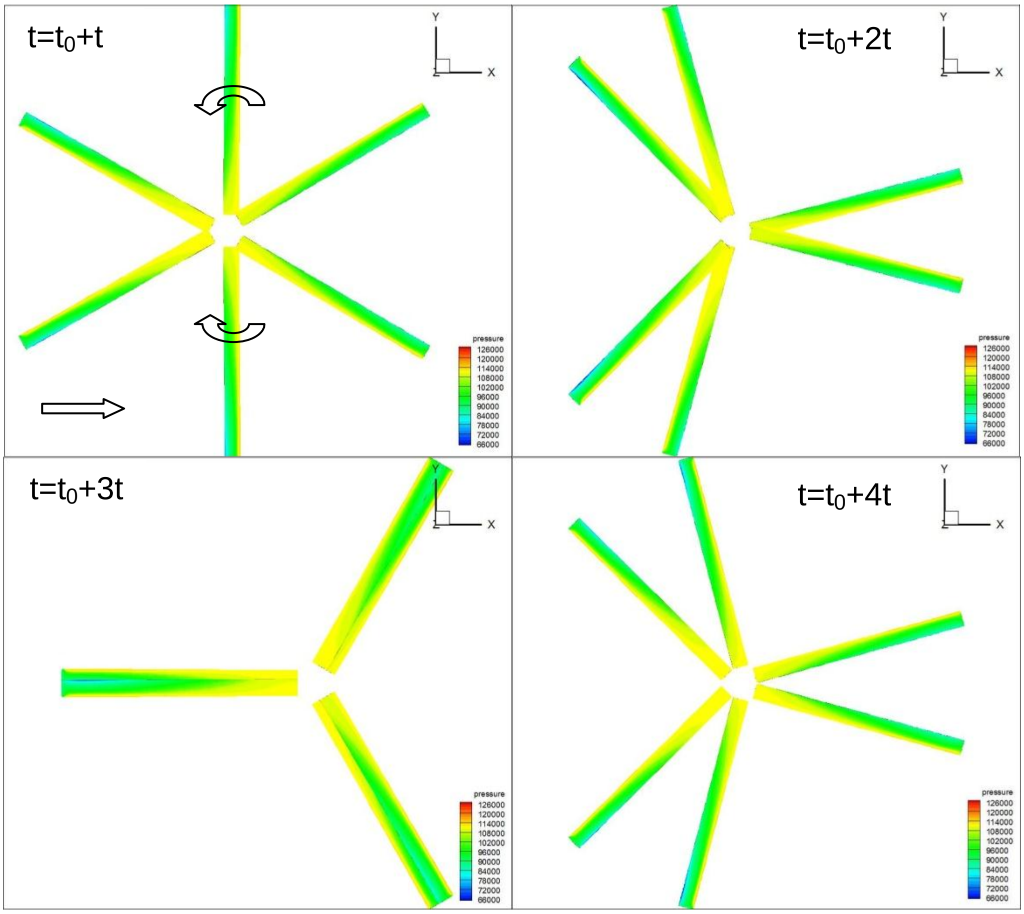

Figure 11: *Pressure contours on the lower and upper rotors at different time steps, forward flight, η=0.1, M_{tip}=0.52, Spalart–Allmaras*

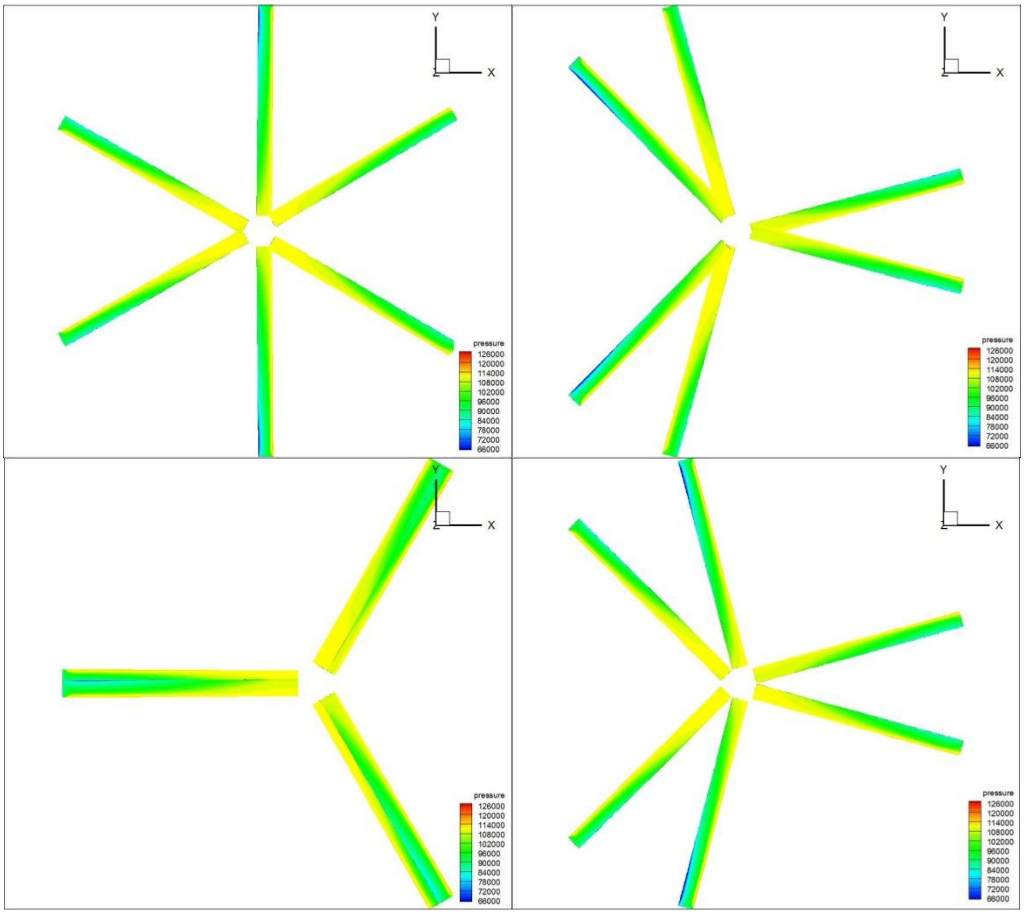

Figure 12: *Pressure contours on the lower and upper rotors at different time steps, forward flight, η=0.2, M_{tip}=0.52, Spalart–Allmaras*

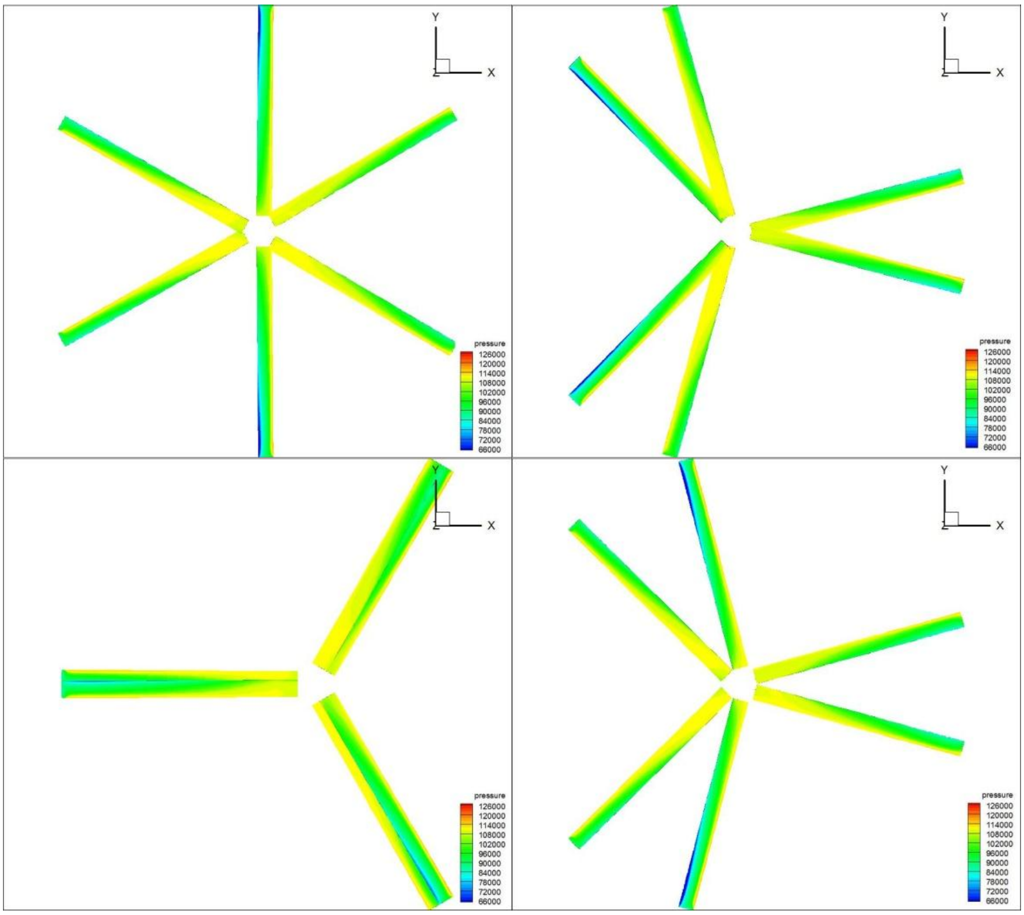

Figure 13: *Pressure contours on the lower and upper rotors at different time steps, forward flight, η=0.3, M_{tip}=0.52, Spalart–Allmaras*

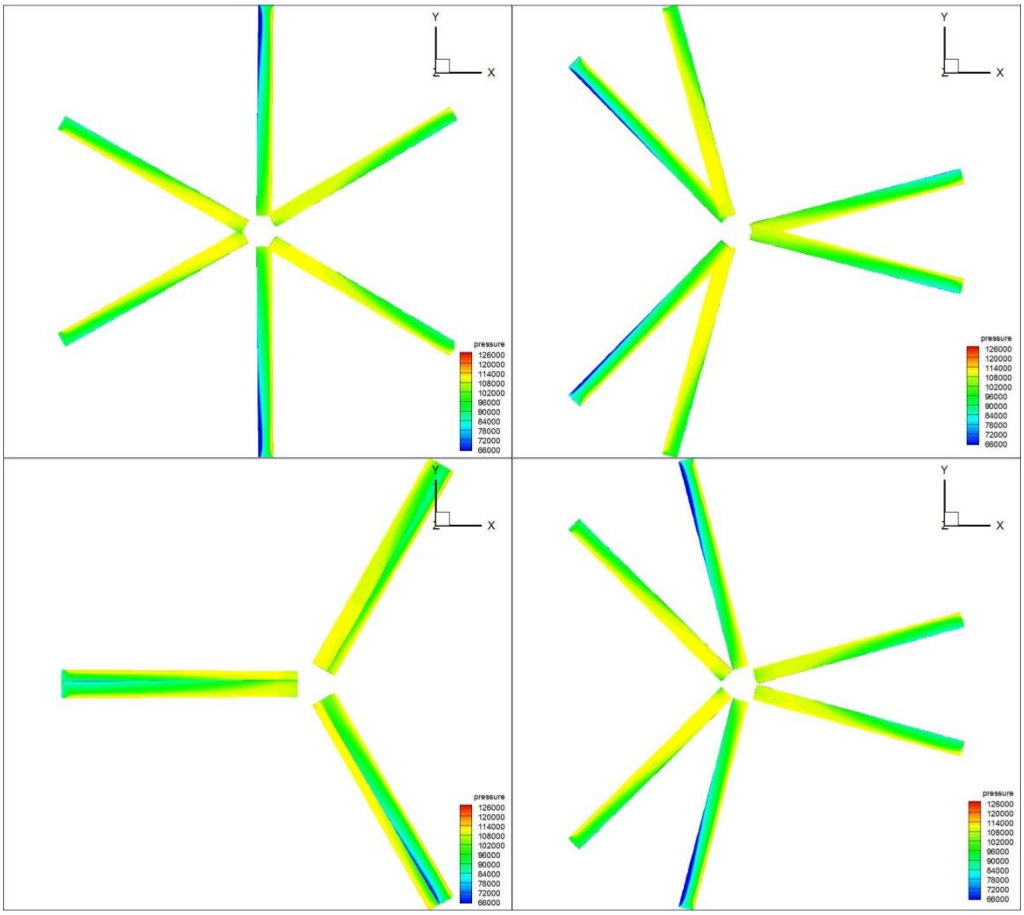

Figure 14: *Pressure contours on the lower and upper rotors at different time steps, forward flight, η=0.4, M_{tip}=0.52, Spalart–Allmaras*

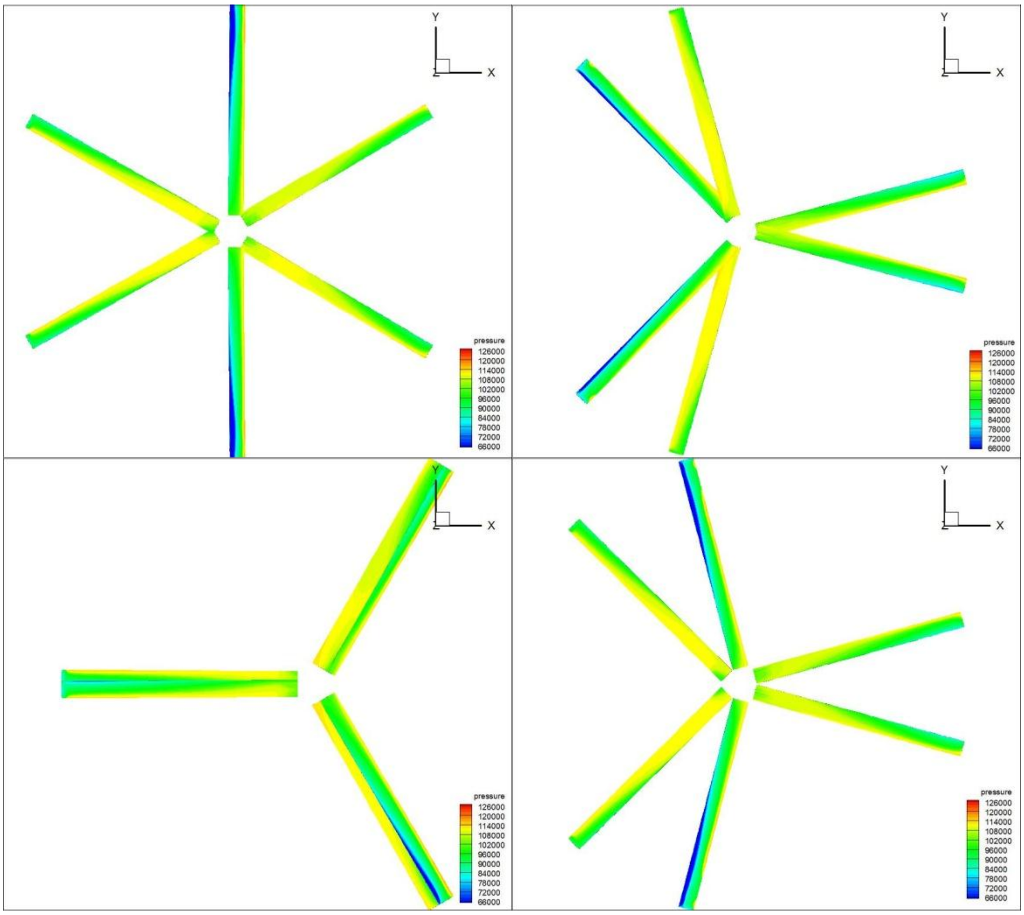

Figure 15: *Pressure contours on the lower and upper rotors at different time steps, forward flight, η=0.5, Mtip=0.52, Spalart–Allmaras*

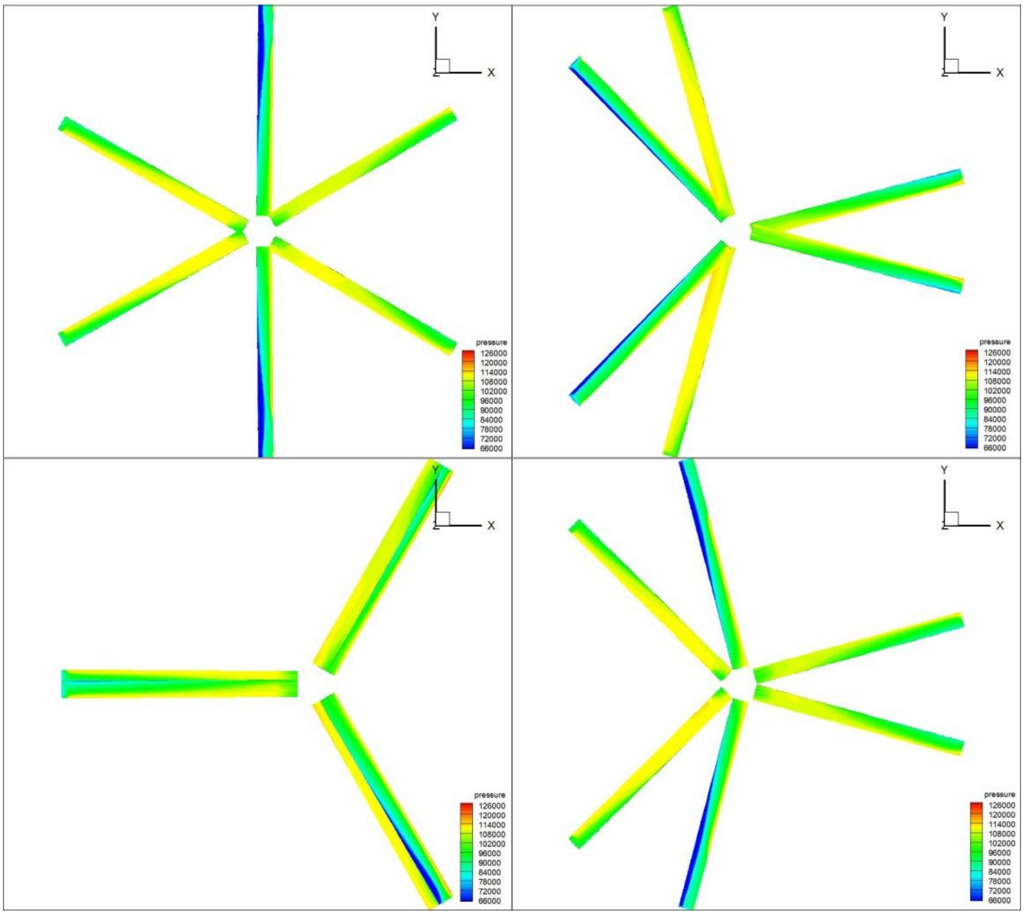

Figure 16: *Pressure contours on the lower and upper rotors at different time steps, forward flight, η=0.6, M_{tip}=0.52, Spalart–Allmaras*

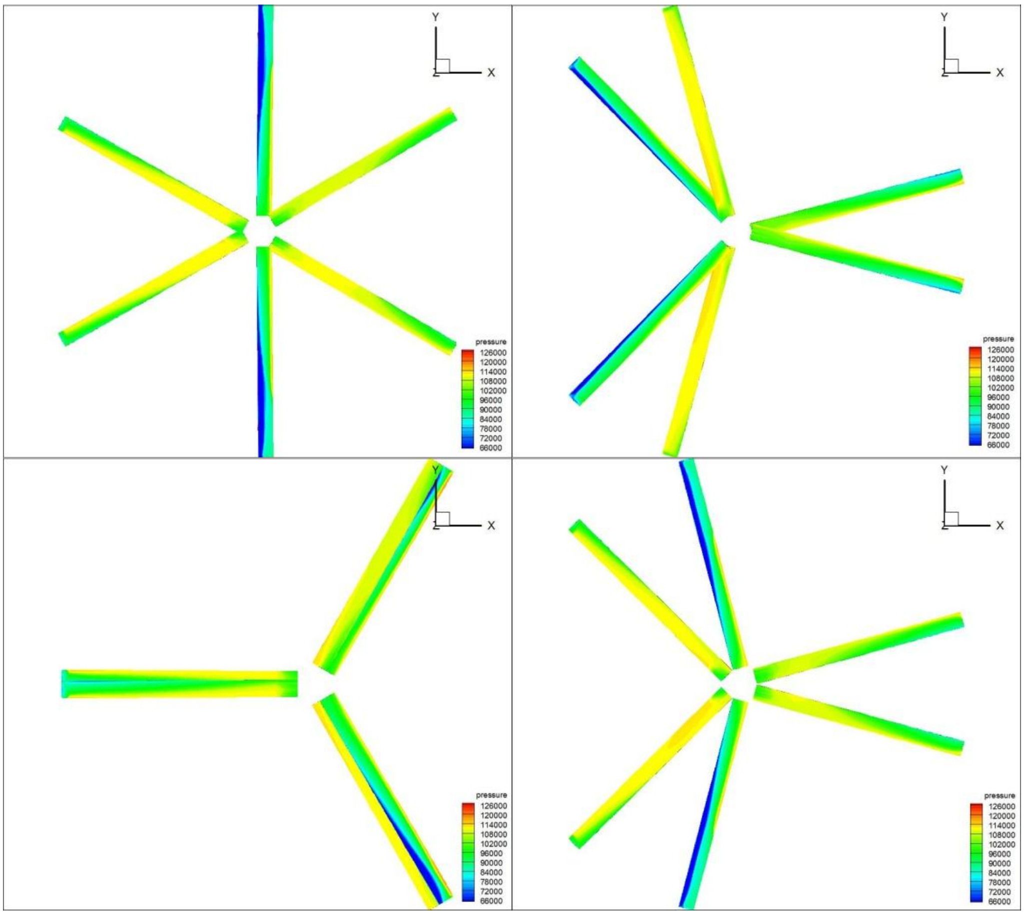

Figure 17: *Pressure contours on the lower and upper rotors at different time steps, forward flight, η=0.7, M_{tip}=0.52, Spalart–Allmaras*

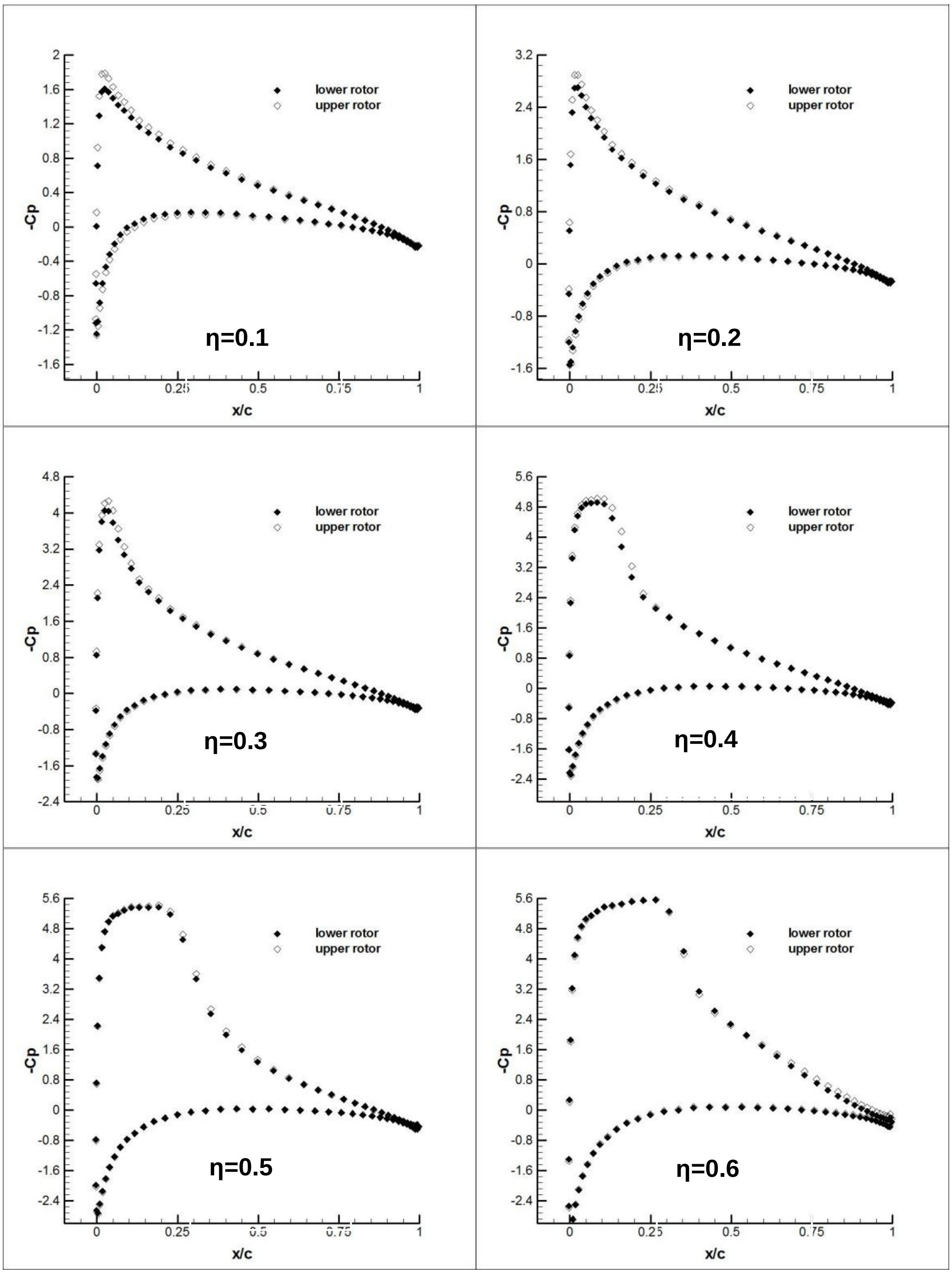

Figure 18: *Comparison of C_p distributions at r/R=0.80 on the lower and upper rotors, forward flight, M_{tip}=0.52, Spalart–Allmaras*

In Figures 11-17, the effect of increasing forward speed can be easily observed. The figures show the instantaneous pressure contours at $t=t_0+t$ (up, left), $t=t_0+2t$ (up, right) $t=t_0+3t$ (low, left) and $t=t_0+4t$ (low, right). At $t=t_0+t$, an aerodynamic symmetry has been observed for each forward speed case. In Figure 16 a comparison of the section pressure coefficient distributions have been displayed. Pressure values on the lower and upper rotor surfaces are almost equal. Therefore, it may be concluded that aerodynamic symmetry has been achieved by the coaxial rotor configuration at different forward flight speeds.

Effect of Rotor Separation Distance on Lift

In this section of the present study, the effect of the rotor separation distance on the lift produced by the upper and the lower rotors has been investigated. For this purpose, five grids with different rotor separation distances have been generated. Simulations have been performed for these five H/D values (0.18, 0.19, 0.20, 0.21 and 0.22).

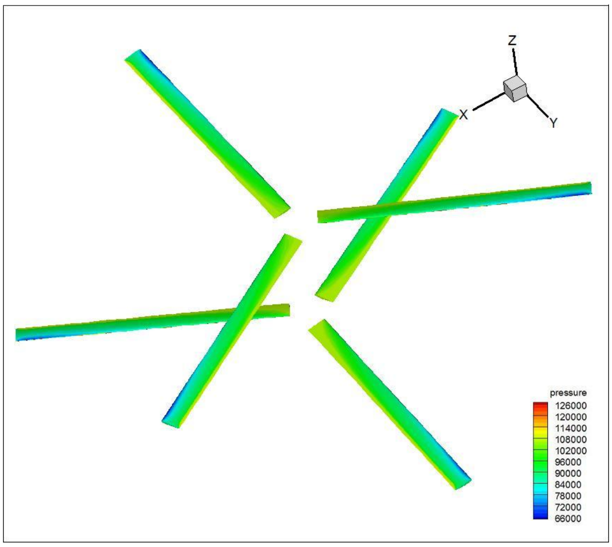

Figure 19: *Pressure contours on the upper and lower rotors, hover, H/D=0.18*

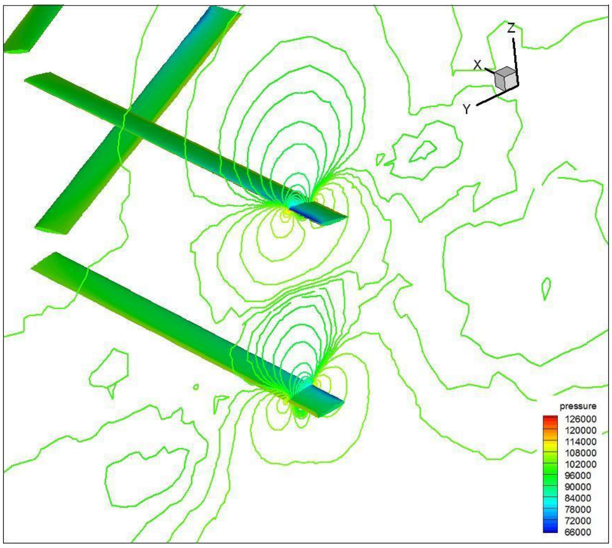

Figure 20: *Interaction between the upper and lower rotors; pressure contours at r/R=0.89, $\psi=270^o$, H/D=0.20*

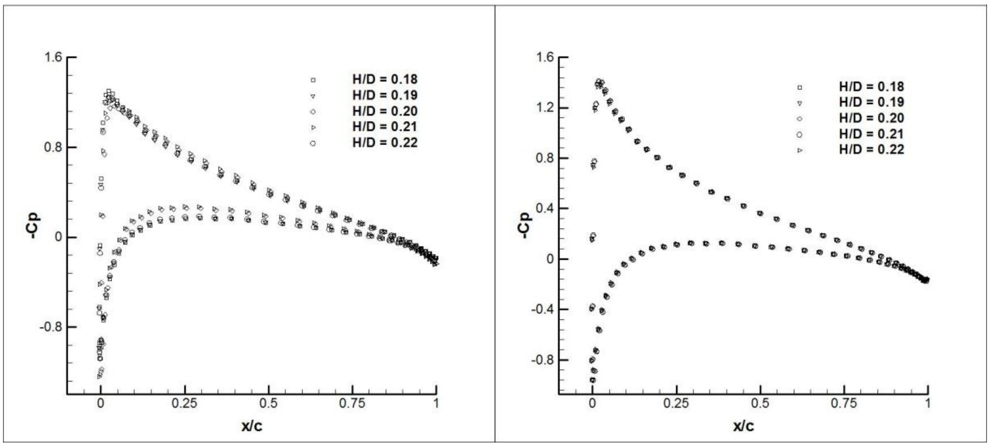

Figure 21: *Comparison of C_p distributions on the* ***lower*** *(left) and* ***upper*** *(right) surfaces for 5 H/D values, hover, M_{tip}=0.52, Spalart–Allmaras*

Figure 21 displays the pressure coefficient distributions on lower and upper surfaces for 5 H/D values. No significant difference has been observed between the pressure values on the lower surface. However, there seems to be a small difference for H/D = 0.20 and 0.21 cases. On the upper surface, the pressure values seem to be identical for all the tested H/D cases.

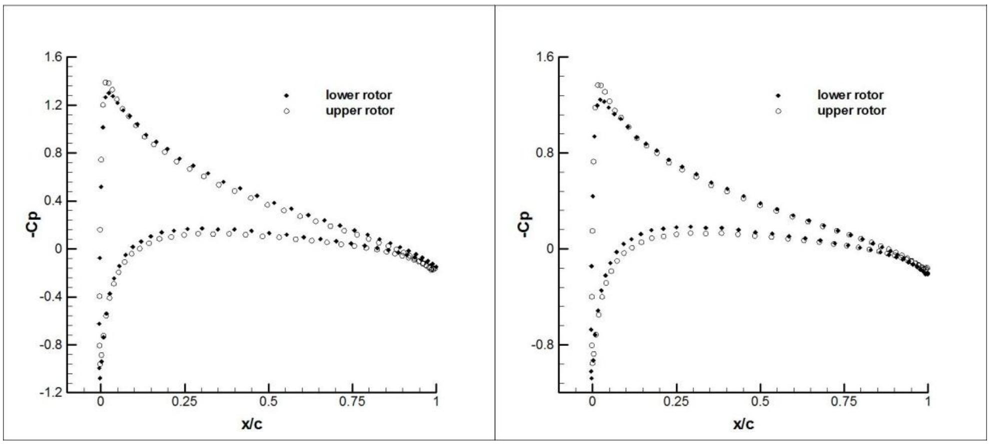

Figure 22: *C_p distributions on the upper and lower rotors, H/D=0.1 (left) and H/D=0.5 (right) hover, M_{tip}=0.52, Spalart–Allmaras*

In Figure 22, pressure values on lower and upper surfaces are compared for H/D=0.1 and H/D=0.5 values. These results seem to suggest that the change in the H/D value does not have a significant effect on the lift produced.

Conclusions and Future Work

A framework for rotorcraft analysis has been developed, validated and utilized for the prediction of aerodynamics of single and coaxial helicopter rotors. In order to understand the suitability of the model and its solver for the problem at hand, a series of comparisons have been obtained between the results and previously published results. The validation cases have been designed so to compare with the experimental data obtained by Caradonna and Tung (1981). Inviscid then laminar viscous results have been obtained where the C_p values at three span wise stations have been compared. It has been concluded that the overall agreement with the experimental data has been deemed satisfactory. To decide on the suitable turbulence model to be employed in the simulations, various turbulence models have been tested. Among the models that have produced successful results, only Spalart-Allmaras is a one-equation model. Since that would translate into being computationally the most efficient, the Spalart-Allmaras model has been chosen to be utilized in the simulations. In order to verify the aerodynamic symmetry proposed by the "Advancing Blade Concept", a hybrid mesh (H/D=0.2) has been utilized and simulations have been performed for 7 different forward flight speeds. Indeed, aerodynamic symmetry has been successfully achieved for all forward flight speeds. In the final part of the present study, the effect of rotor separation distance (H/D) on lift has been investigated. 5 different grids have been generated by setting the H/D value to 0.18, 0.19, 0.20, 0.21 and 0.22. Then, the obtained C_p values on the upper and lower rotors have been compared. For these cases, either small or almost no effect on lift has been observed.

The present investigation has been conducted for constant collective angles for both the lower and the upper rotors. Future simulations with independently changing lower and upper rotor collective angles will be helpful to better understand the aerodynamics of coaxial rotors. Including the fuselage in the model should also have noticeable effect on the flowfield generated by the rotors. Therefore, generating a mesh for a domain that includes the rotor and the fuselage should result in more realistic predictions. Furthermore, effect of phase shift between rotors for optimal operation has not been examined in the current study. Conducting simulations with changing phase angles between the rotors should help one to design more effective coaxial rotor configurations. Vertical pitch of vortex per revolution has not been considered in the surveys. In order to minimize the BVI noise, particularly for coaxial rotor configurations, observation of the vertical pitch per revolution may also be useful. Moreover, a parametric study to analyze the effects of changing blade number, planform shape, rotor solidity and section profile may be a valuable contribution to the computational analyses of coaxial rotor configurations.

References

Allen, C.B. (2007) *Parallel Simulation of Lifting Rotor Wakes in Forward Flight*, International Journal Of Numerical Analysis And Modeling Volume 4, Number 1, Pages 1–15, 2007, Institute for Scientific Computing and Information.

Altmikus, A.R.M., Wagner, S., Beaumier, P. and Servera, G. (2002) *A Comparison: Weak Versus Strong Modular Coupling for Trimmed Aeroelastic Rotor Simulations*, American Helicopter Society 58th Annual Forum, Montreal, Quebec, June 2002.

Boelens, O.J., Van der Ven, H., Oskam, B. and Hassan, A.A. (2002) *Boundary Conforming Discontinuous Galerkin Finite Element Approach for Rotorcraft Simulations*, Journal of Aircraft 2002; 39(5): 776–785.

Caradonna, F. X. and Tung, C. (1981) *Experimental and Analytical Studies of a Model Helicopter Rotor in Hover*, NASA Technical Memorandum 81: 232, September 1981.

Cheney, M.C. (1969) *The ABC Helicopter*, Presented at the AIAA/AHS VTOL Research, Design and Operations Meeting, Atlanta, GA., February 17–19, 1969.

Coleman, C.P. (1997) *A Survey of Theoretical and Experimental Coaxial Rotor Aerodynamic Research*, NASA Technical Paper 3675, March 1997.

Conlisk, A.T. (2001) *Modern Helicopter Rotor Aerodynamics*, Progress in Aerospace Sciences 37 (2001) 419–476.

Fluent Inc. (2006) *Fluent 6.3 User's Guide*, © Fluent Inc. 2006-09-20.

Le Pape, A. and Beaumier, P. (2005) *Numerical Optimization of Helicopter Rotor Aerodynamic Performance in Hover*, Aerospace Science and Technology 9 (2005) 191–201.

Leishman, J.G. (2006) *Principles of Helicopter Aerodynamics*, Cambridge University Press, 2006.

Park, Y. and Kwon, O. (2004) *Simulation of Unsteady Rotor Flow Field Using Unstructured Adaptive Sliding Meshes,* Journal of the American Helicopter Society 2004; 49(4):391–400.

Pomin, H. and Wagner, S. (2001) *Navier–Stokes Analysis of Helicopter Rotor Aerodynamics in Hover and Forward Flight*, Journal of Aircraft 39 (5), 813–821, Presented as Paper 2001–0998 at the AIAA 39th Aerospace Sciences Meeting & Exhibit, Reno, NV, January 2001.

Rouzaud, O., Raddatz, J. and Boniface, J.C. (1997) *Euler Calculations of Multibladed Rotors in Hover by DLR and ONERA Methods and Comparison with Helishape Tests*, American Helicopter Society 53rd Annual Forum, Virginia Beach, 29 April–1 May 1997.

Servera, G., Beaumier, P. and Costes, M. (2001) *A Weak Coupling Method Between The Dynamics Code HOST and the 3D Unsteady Euler Code WAVES*, Aerospace Science and Technology 2001; 5:397–408.

Steijl, R., Barakos, G. and Badcock, K. (2006) *A Framework For CFD Analysis of Helicopter Rotors in Hover and Forward Flight*, International Journal For Numerical Methods in Fluids 2006; 51:819–847.

Strawn, R. and Biswas, R. (1994) *Computation of Helicopter Rotor Acoustics in Forward Flight*, Presented at the 19th Army Science Conference, 20-24 June, 1994, Orlando, Florida.

Sheffer, S.G., Alonso, J.J., Martinelli, L. and Jameson, A. (1997) *Time-Accurate Simulation of Helicopter Rotor Flows Including Aeroelastic Effects*, AIAA, Aerospace Sciences Meeting & Exhibit, 35th, Reno, NV, Jan. 6-9, 1997.

Srinivasan, G.R., Raghavan, V. and Duque, E. P. N. (1991) *Flowfield Analysis of Modern Helicopter Rotors in Hover by Navier–Stokes Method*, International Technical Specialist Meeting, Rotorcraft Acoustics and Rotor Fluid Dynamics, October 15-17, 1991, Philadelphia, Pennsylvania, USA.

Van der Ven, H. and Boelens, O.J. (2004) *A Framework For Aeroealistic Simulations of Trimmed Rotor Systems in Forward Flight,* European Rotorcraft Forum, Marseille, September 14–16, 2004.

Xu, H., Zhang, S. and Khalid, M.(2005) *Numerical Simulations of Unsteady Flows Past a Four-Bladed Rotor in Forward-Flight*, AIAA 17th Computational Fluid Dynamics Conference, Toronto, Canada, AIAA Paper 2005–5125.

Yang, Z., Sankar, L.N., Smith, M. and Bauchau, O. (2000) *Recent Improvements to a Hybrid Method for Rotors in Forward Flight*, Journal of Aircraft 39 (5), 804–812, Presented as Paper 2000–0260 at the AIAA 38th Aerospace Sciences Meeting & Exhibit, Reno, NV, January 2000.